

Jupiter’s Dynamical Love Number

DONG LAI¹

¹*Cornell Center for Astrophysics and Planetary Science, Department of Astronomy, Cornell University, Ithaca, NY 14853*

Abstract

Recent observations by the *Juno* spacecraft have revealed that the tidal Love number k_2 of Jupiter is 4% lower than the hydrostatic value. We present a simple calculation of the dynamical Love number of Jupiter that explains the observed “anomaly”. The Love number is usually dominated by the response of the (rotation-modified) f-modes of the planet. Our method also allows for efficient computation of high-order dynamical Love numbers. While the inertial-mode contributions to the Love numbers are negligible, a sufficiently strong stratification in a large region of the planet’s interior would induce significant g-mode responses and influence the measured Love numbers.

Keywords: dynamical tides — giant planets — Jupiter’s interior — gravitational fields

1. INTRODUCTION

The *Juno* spacecraft recently found an “anomaly” in Jupiter’s tidal Love number: the measured $k_2 = 0.565 \pm 0.006$ (Durante et al. 2020) appears to be smaller than the theoretical hydrostatic value $k_2^{(\text{hs})} = 0.590$ (Wahl et al. 2020) by 4%. This discrepancy may be explained in terms of dynamical tides, i.e., Jupiter’s response to the finite-frequency tidal forcings from the Galilean moons (Idini & Stevenson 2021). Here we present a simple calculation that explains this Love number “anomaly” quantitatively. Naive expectation would suggest a $1/(\omega_\alpha^2 - \omega^2)$ enhancement (where ω_α is the f-mode frequency of the planet) of the tidal response due to the finite tidal frequency (ω) as compared to the hydrostatic ($\omega = 0$) response. The key to obtain the correct answer is to treat the rotational (Coriolis) effect on the modes of a rotating planet and their tidal responses in a self-consistent way. Our general method also allows for efficient computation of high-order dynamical Love numbers k_{lm} , as well as the inclusion of the contributions to k_{lm} from the inertial modes (due to planetary rotation) and g-modes (due to stable stratification in the planetary interior).

2. DYNAMICAL LOVE NUMBER AND NORMAL MODES

Consider a planet (mass M , radius R and spin angular frequency Ω_s) orbited by a satellite (mass M') in a circular orbit with semi-major axis a and orbital frequency Ω_{orb} . We assume the spin axis is aligned with the orbital axis. In the frame corotating with the planet, the (lm) -component of the tidal potential produced by M'

on the planet is

$$U(\mathbf{r}, t) = -A_{lm} r^l Y_{lm}(\theta, \phi) e^{-i\omega t}, \quad (1)$$

where $A_{lm} = (GM'/a^{l+1})W_{lm}$ (with W_{lm} a dimensionless constant; $W_{lm} \neq 0$ when $l + m = \text{even}$), $\mathbf{r} = (r, \theta, \phi)$ specifies the position vector (in spherical coordinates) measured from the center of the planet, and

$$\omega = m(\Omega_{\text{orb}} - \Omega_s) \quad (2)$$

is the tidal forcing frequency. It suffices to consider only $m > 0$. The relevant non-zero tidal components are $(lm) = (2, 2), (3, 1), (3, 3), (4, 2), (4, 4)$ etc.

The linear response of the planet to the tidal forcing is specified by the Lagrangian displacement, $\boldsymbol{\xi}(\mathbf{r}, t)$, of a fluid element from its unperturbed position. In the rotating frame of the planet, the equation of motion takes the form

$$\frac{\partial^2 \boldsymbol{\xi}}{\partial t^2} + 2\boldsymbol{\Omega}_s \times \frac{\partial \boldsymbol{\xi}}{\partial t} + \mathbf{C} \cdot \boldsymbol{\xi} = -\nabla U, \quad (3)$$

where \mathbf{C} is a self-adjoint operator (a function of the pressure and gravity) acting on $\boldsymbol{\xi}$ (see, e.g., Friedman & Schutz 1978). A free mode of frequency ω_α (in the rotating frame) with $\boldsymbol{\xi}_\alpha(\mathbf{r}, t) = \boldsymbol{\xi}_\alpha(\mathbf{r}) e^{-i\omega_\alpha t} \propto e^{im\phi - i\omega_\alpha t}$ satisfies

$$-\omega_\alpha^2 \boldsymbol{\xi}_\alpha - 2i\omega_\alpha \boldsymbol{\Omega}_s \times \boldsymbol{\xi}_\alpha + \mathbf{C} \cdot \boldsymbol{\xi}_\alpha = 0, \quad (4)$$

where $\{\alpha\}$ denotes the mode index, which includes the azimuthal number m . We carry out phase-space mode expansion (Schenk et al. 2002)

$$\left[\begin{array}{c} \boldsymbol{\xi} \\ \partial \boldsymbol{\xi} / \partial t \end{array} \right] = \sum_{\alpha} c_{\alpha}(t) \left[\begin{array}{c} \boldsymbol{\xi}_{\alpha}(\mathbf{r}) \\ -i\omega_{\alpha} \boldsymbol{\xi}_{\alpha}(\mathbf{r}) \end{array} \right]. \quad (5)$$

Using the orthogonality relation $\langle \xi_\alpha, 2i\Omega_s \times \xi_{\alpha'} \rangle + (\omega_\alpha + \omega_{\alpha'}) \langle \xi_\alpha, \xi_{\alpha'} \rangle = 0$ (for $\alpha \neq \alpha'$), where $\langle A, B \rangle \equiv \int d^3x \rho (A^* \cdot B)$, we find (Lai & Wu 2005)

$$\dot{c}_\alpha + i\omega_\alpha c_\alpha = \frac{iQ_{\alpha,lm}}{2\varepsilon_\alpha} A_{lm} e^{-i\omega t}, \quad (6)$$

where

$$Q_{\alpha,lm} \equiv \langle \xi_\alpha, \nabla(r^l Y_{lm}) \rangle = \int d^3x r^l Y_{lm} \delta\rho_\alpha^*, \quad (7)$$

$$\varepsilon_\alpha \equiv \omega_\alpha + \langle \xi_\alpha, i\Omega_s \times \xi_\alpha \rangle, \quad (8)$$

and we have used the normalization $\langle \xi_\alpha, \xi_\alpha \rangle = 1$. In Eq. (7), $\delta\rho_\alpha$ is the Eulerian density perturbation associated with the eigenfunction ξ_α .

Equation (6) has stationary solution

$$c_\alpha(t) = \frac{Q_{\alpha,lm}}{2\varepsilon_\alpha(\omega_\alpha - \omega)} A_{lm} e^{-i\omega t}. \quad (9)$$

The gravitational perturbation associated with the density perturbation $\delta\rho(\mathbf{r}, t) = \sum_\alpha c_\alpha(t) \delta\rho_\alpha(\mathbf{r})$, evaluated at the planet's surface ($r = R$), is

$$\delta\Phi(\mathbf{r}, t) \Big|_{r=R} = - \sum_\alpha c_\alpha(t) \frac{4\pi}{2l+1} \frac{GMQ_{\alpha,lm}}{R} Y_{lm}. \quad (10)$$

Thus the tidal Love number is

$$k_{lm} = \frac{\delta\Phi}{U} \Big|_{r=R} = \frac{2\pi}{2l+1} \sum_\alpha \frac{\bar{Q}_{\alpha,lm}^2}{\bar{\varepsilon}_\alpha(\bar{\omega}_\alpha - \bar{\omega})}. \quad (11)$$

In the above equation, the tidal overlap coefficient $\bar{Q}_{\alpha,lm}$ and the mode frequencies $\bar{\omega}_\alpha$ and $\bar{\varepsilon}_\alpha$ are in units where $G = M = R = 1$, i.e., $\bar{\omega}_\alpha = \omega_\alpha / (GM/R^3)^{1/2}$, etc. Note that for a given $m > 0$, the sum in Eq. (11) includes modes with positive ω_α and negative ω_α , corresponding to prograde (with respect to the planet's rotation) and retrograde modes.

3. F-MODE CONTRIBUTION

In most situations, the sum in Eq. (11) is dominated by f-modes since they have the largest tidal overlap $Q_{\alpha,lm}$. For planetary rotation rate Ω_s much less than the breakup rate $(GM/R^3)^{1/2}$, (e.g., $\bar{\Omega}_s = 0.288$ for Jupiter), the effect of rotation on the modes can be treated perturbatively (e.g. Unno et al. 1989). Let ω_0 (> 0) be the mode frequency of a non-rotating planet, then for a given $m > 0$, the sum in Eq. (11) includes

$$\varepsilon_\alpha \simeq \pm\omega_0, \quad (12)$$

$$\omega_\alpha = \pm\omega_0 - mC\Omega_s, \quad (13)$$

with

$$\begin{aligned} mC &\equiv \int d^3x \rho \xi_{\alpha,0}^* \cdot (i\hat{\mathbf{z}} \times \xi_{\alpha,0}) \\ &= m \int_0^R dr \rho r^2 (2\xi_r \xi_\perp + \xi_\perp^2), \end{aligned} \quad (14)$$

Table 1. Oscillation modes of non-rotating polytropic ($n = 1$) planet model

| | | ω_0 | Q_l | C |
|------------------|-----|----------------------|----------------|------------|
| $\Gamma_1 = 2$ | | | | |
| $l = 2$ | f | 0.1227E+01 | 0.5579E+00 | 0.4991E+00 |
| | p1 | 0.3462E+01 | 0.2690E-01 | 0.1119E+00 |
| $l = 3$ | f | 0.1698E+01 | 0.5846E+00 | 0.3321E+00 |
| | p1 | 0.3975E+01 | 0.4054E-01 | 0.8627E-01 |
| $l = 4$ | f | 0.2037E+01 | 0.5979E+00 | 0.2489E+00 |
| | p1 | 0.4409E+01 | 0.4623E-01 | 0.6984E-01 |
| $\Gamma_1 = 2.4$ | | | | |
| $l = 2$ | f | 0.1230E+01 | 0.5580E+00 | 0.4985E+00 |
| | g1 | 0.4688E+00 | -0.1313E-01 | 0.1057E+00 |
| | g2 | 0.3270E+00 | 0.3071E-02 | 0.1342E+00 |
| | g3 | 0.2526E+00 | -0.8961E-03 | 0.1464E+00 |
| $l = 3$ | f | 0.1703E+01 | 0.5850E+00 | 0.3317E+00 |
| | g1 | 0.5681E+00 | -0.1216E-01 | 0.3321E-01 |
| | g2 | 0.4117E+00 | 0.3257E-02 | 0.5622E-01 |
| | g3 | 0.3254E+00 | -0.1031E-02 | 0.6603E-01 |
| $\Gamma_1 = 2.4$ | for | $r \in [0.5, 0.7]$, | $[0.85, 0.93]$ | |
| $l = 2$ | f | 0.1228E+01 | 0.5580E+00 | 0.4988E+00 |
| | g1 | 0.3664E+00 | -0.6986E-02 | 0.9279E-01 |
| | g2 | 0.2022E+00 | 0.1408E-02 | 0.1207E+00 |
| | g3 | 0.1565E+00 | -0.1546E-03 | 0.1467E+00 |
| $l = 3$ | f | 0.1701E+01 | 0.5849E+00 | 0.3319E+00 |
| | g1 | 0.4489E+00 | -0.6067E-02 | 0.2790E-01 |
| | g2 | 0.2749E+00 | 0.2049E-02 | 0.4166E-01 |
| | g3 | 0.2126E+00 | -0.1567E-03 | 0.6622E-01 |

NOTE— ω_0 and Q_l are the mode frequency and tidal overlap coefficient (Eq. 7), both in units such that $G = M = R = 1$, and C is defined in Eq. (14). The planet's density profile is that of $n = 1$ polytrope (with the equation of state $P \propto \rho^2$). The first model has Γ_1 (the adiabatic index) equal to $\Gamma = 1 + 1/n$, and we list the properties for the f-mode and the first radial-order p-mode. The second model has $\Gamma_1 = 2.4$ throughout the planet, and the third model has $\Gamma_1 = 2.4$ only in two regions ($r/R \in [0.5, 0.7]$, $[0.85, 0.93]$) and $\Gamma_1 = \Gamma$ otherwise (the transition width is $0.025R$; see Eq. 26), and we list the properties for the f-mode and the first three radial-order g-modes. Note that when $|Q_l| \ll 1$, the quoted Q_l values are only accurate in 2-3 significant figures.

where $\xi_{\alpha,0} = [\xi_r(r)\hat{\mathbf{r}} + \xi_\perp(r)r\nabla_\perp] Y_{lm}$ is the mode eigenvector of a non-rotating planet. To a good approximation, we can also set $Q_{\alpha,lm}$ to be the non-rotating value, i.e.,

$$Q_{\alpha,lm} \simeq Q_l. \quad (15)$$

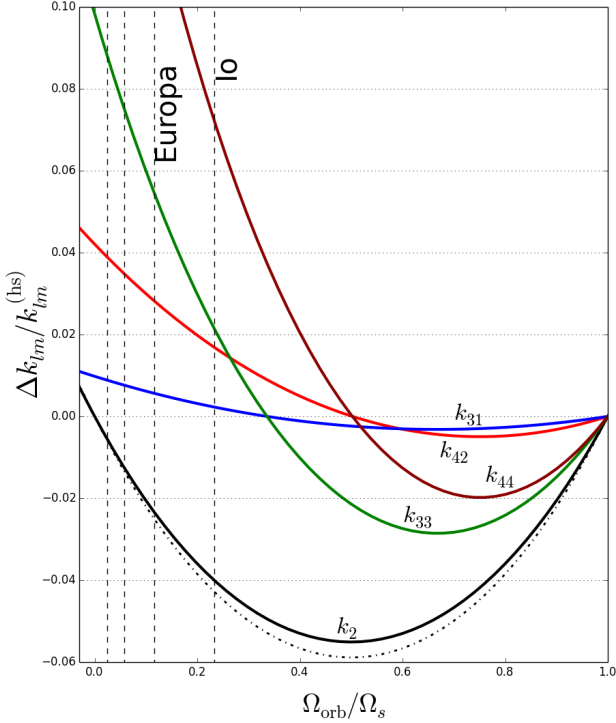


Figure 1. Dynamical correction $\Delta k_{lm}/k_{lm}^{(hs)} = (k_{lm} - k_{lm}^{(hs)})/k_{lm}^{(hs)}$ to Jupiter’s tidal Love number as a function of the orbital frequency Ω_{orb} of the perturbing satellite (in units of the spin frequency Ω_s). All results (solid curves) are computed using the $n = 1$ (isentropic) polytrope model, except that the dot-dashed curve is for $k_2 = k_{22}$ computed using the $n = 0.9$ polytrope model. The vertical dashed lines specify the orbital frequencies of Io, Europa, Ganymede and Callisto (from right to left). The -4% “anomaly” of k_2 observed by *Juno* can be explained by the planetary model with $n \simeq 1$.

Thus Eq. (11) reduces to

$$k_{lm} \simeq \left(\frac{4\pi}{2l+1} \right) \frac{\bar{Q}_l^2}{\bar{\omega}_0^2 - (mC\Omega_s + \bar{\omega})^2}. \quad (16)$$

For an incompressible planet model ($n = 0$ polytrope), the $l = 2$ mode (Kelvin mode) has

$$\bar{\omega}_0 = \frac{2}{\sqrt{5}}, \quad \bar{Q}_2 = \left(\frac{3}{2\pi} \right)^{1/2}, \quad C = \frac{1}{2}. \quad (17)$$

Thus

$$k_2 \equiv k_{22} \simeq \frac{3}{2} \left[1 - \frac{5}{4} (\bar{\Omega}_s + \bar{\omega})^2 \right]^{-1}, \quad (18)$$

with $\bar{\omega} = 2(\bar{\Omega}_{orb} - \bar{\Omega}_s)$.

Giant planets are approximately described by a $n = 1$ polytrope (corresponding to $P \propto \rho^2$). Table 1 list the numerical values of ω_0 , Q_l and C for several non-rotating poltropic models (with different levels of stratification; see Section 5). For $l = m = 2$ tidal response

(and $n = 1$), $2C \simeq 1$, we have

$$k_2 \simeq 0.520 \left[1 - 0.664(\bar{\Omega}_s + \bar{\omega})^2 \right]^{-1}. \quad (19)$$

Applying to the Jupiter-Io system: Jupiter has $\bar{\Omega}_s = 0.288$ [with spin period 9.925 hrs and $2\pi(R^3/GM)^{1/2} = 2.863$ hrs], Io has $\bar{\Omega}_{orb} = 0.0674$ (orbital period 1.769 days), so $\bar{\omega} = -0.441$. Thus the hydrostatic and dynamical k_s values are

$$k_2^{(hs)} = 0.550, \quad k_2 = 0.528 = 0.960 k_2^{(hs)} \quad (20)$$

This explains the 4% discrepancy between k_2 and $k_2^{(hs)}$. Note that our static $k_2^{(hs)}$ does not agree with the value (0.590) from Wahl et al. (2020). This could arise for two reasons: (i) The simple $n = 1$ polytropic model does not precisely represent Jupiter’s internal structure; (ii) In deriving Eq. (16), we have neglected order $\bar{\Omega}_s^2$ corrections to the mode frequency and the tidal overlap¹.

Figure 1 shows the dynamical corrections $\delta_{lm} \equiv \Delta k_{lm}/k_{lm}^{(hs)} = (k_{lm} - k_{lm}^{(hs)})/k_{lm}^{(hs)}$ to Jupiter’s tidal Love numbers as a function of the orbital frequency Ω_{orb} of the perturbing satellite. These results are obtained using the $n = 1$ isentropic model, which gives the hydrostatic values $k_{lm}^{(hs)} \simeq 0.550, 0.213, 0.219, 0.121, 0.123$ for $(lm) = (22), (31), (33), (42), (44)$, respectively. Although these hydrostatic values may not correspond to the “true” values for Jupiter because of the simplicity of the polytrope model and the $\bar{\Omega}_s^2$ corrections (see above), the dynamical corrections δ_{lm} shown in Fig. 1 are robust.

Our results depicted in Fig. 1 can be compared to those of Idini & Stevenson (2021) obtained using more complicated calculations (see their Table 2). Our δ_{22} , δ_{33} and δ_{44} values (evaluated for the orbital frequencies of Io, Europa, Ganymede and Callisto) agree reasonably well with theirs, but our δ_{31} , δ_{42} values are a factor of a few smaller.

Finally, using Table 1, we can easily check that the contributions from p-modes to k_{lm} are negligible.

4. INERTIAL-MODE CONTRIBUTION

In addition to f-modes and p-modes, a rotating planet possesses a spectrum of inertial modes supported by Coriolis force.

¹ Both $\bar{\omega}_0^2$ and \bar{Q}_l^2 in Eq. (16) can have corrections of order $\bar{\Omega}_s^2$. These corrections do not affect $\Delta k_2/k_2^{(hs)}$ to the leading order. Note that for $n = 0$ (incompressible MacLaurin spheroid), the exact expressions for the mode frequency and tidal overlap coefficient are available [see Eq. (3.4) and Eq. (3.22) of Ho & Lai (1999)].

For $n = 1$ polytrope, the $m = 2$ inertial modes have been computed by Xu & Lai (2017) using a spectral code. The mode properties are

$$\omega_+ = 0.556\Omega_s, \quad \varepsilon_+ = 0.28\Omega_s, \quad \bar{Q}_+ = 0.015\bar{\Omega}_s^2 \quad (21)$$

for the prograde mode, and

$$\omega_- = -1.10\Omega_s, \quad \varepsilon_- = -0.55\Omega_s, \quad \bar{Q}_- = 0.010\bar{\Omega}_s^2 \quad (22)$$

for the retrograde mode, where Q_{\pm} is the tidal coupling coefficient $Q_{\alpha,22}$. Since $\omega < 0$, we can write the inertial mode contribution of k_2 as

$$k_{2,\text{in}} = \frac{2\pi}{5} \left[\frac{\bar{Q}_+^2}{\bar{\varepsilon}_+(\bar{\omega}_+ + |\bar{\omega}|)} + \frac{\bar{Q}_-^2}{|\bar{\varepsilon}_-(|\bar{\omega}_-| - |\bar{\omega}|)} \right]. \quad (23)$$

Define $\hat{\omega} \equiv \omega/\Omega_s$ (and similarly $\hat{\omega}_{\pm}$ and $\hat{\varepsilon}_{\pm}$) and $\hat{Q}_{\pm} \equiv \bar{Q}_{\pm}/\bar{\Omega}_s^2$, we have

$$k_{2,\text{in}} = \frac{2\pi}{5} \bar{\Omega}_s^2 \left[\frac{\hat{Q}_+^2}{\hat{\varepsilon}_+(\hat{\omega}_+ + |\hat{\omega}|)} + \frac{\hat{Q}_-^2}{|\hat{\varepsilon}_-(|\hat{\omega}_-| - |\hat{\omega}|)} \right]. \quad (24)$$

For $n = 1$ polytrope, this gives

$$k_{2,\text{in}} = \frac{2\pi}{5} \bar{\Omega}_s^2 \times 10^{-4} \left(\frac{8.04}{0.556 + |\hat{\omega}|} + \frac{1.82}{1.10 - |\hat{\omega}|} \right). \quad (25)$$

For Jupiter-Io system, $\hat{\omega} = 2\Omega_{\text{orb}}/\Omega_s - 2 = -1.53$, it is clear that $k_{2,\text{in}} \ll 1$. In general, unless $|\hat{\omega}|$ happens to be very close to $|\hat{\omega}_-|$ (to within 10^{-4}), the contribution of the inertial modes to the Love number is negligible.

5. STABLE STRATIFICATION AND G-MODE CONTRIBUTION

In Sections 3-4 we considered fully isentropic models for Jupiter, i.e., the adiabatic index $\Gamma_1 \equiv (\partial \ln P / \partial \ln \rho)_s$ equals the polytropic index $\Gamma \equiv d \ln P / d \ln \rho = 1 + 1/n$. In reality, some regions of the planet may be stably stratified, with $\Gamma_1 > \Gamma$. Indeed, the gravity measurement by *Juno* and structural modeling suggest that Jupiter have a diluted core and a total heavy-element mass of 10-24 Earth masses, with the heavy elements distributed within an extended region covering nearly half of Jupiter's radius (Wahl et al. 2017; Debras & Chabrier 2019; Stevenson 2020). The composition gradient outside the diluted core would provide stable stratification, and the planet would then possess g-modes. Another stable region may exist between $(0.8-0.9)R$ and $0.93R$ (Debras & Chabrier 2019).

To explore of how g-modes influence the tidal love numbers, we consider three simple planetary models, all having a $n = 1$ density profile ($\Gamma = 2$), but with different adiabatic index profiles: (i) $\Gamma_1 = 2.4$ throughout the

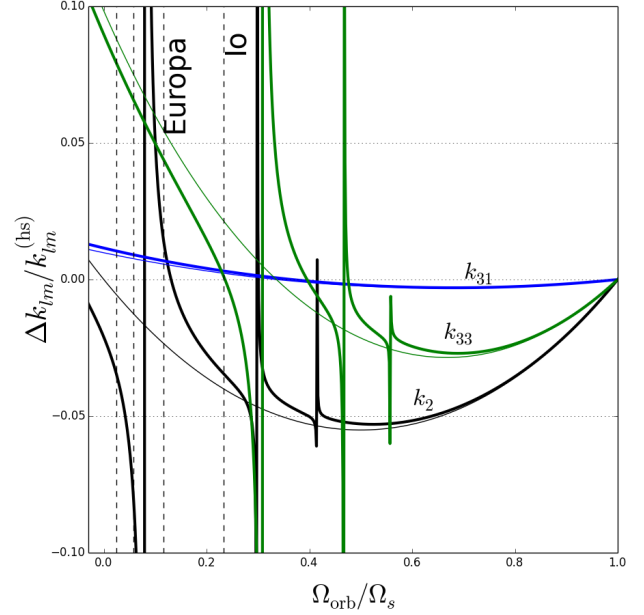


Figure 2. Same as Fig. 1, but for the $n = 1$, $\Gamma_1 = 2.4$ planetary model, which possesses g-modes. The heavy solid curves include the contributions of f-modes and first three radial-order g-modes to k_{lm} , the light solid curves include only f-modes (for the $n = 1$ isentropic model, as in Fig. 1).

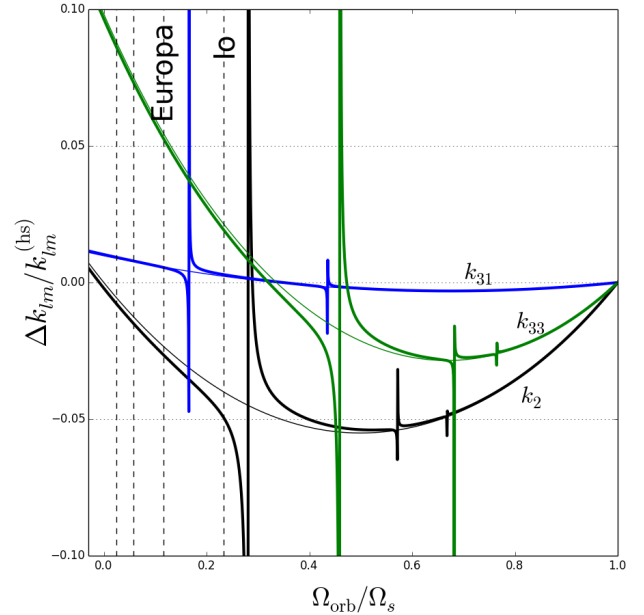


Figure 3. Same as Fig. 2, but for the $n = 1$ model with stable stratification only in the region $r/R \in [0.5, 0.7]$ (see Eq. 26).

planet (see Table 1); (ii) $\Gamma_1 = 2.4$ only in the stable region $\bar{r} = r/R \in [0.5, 0.7]$ (with a transition width of

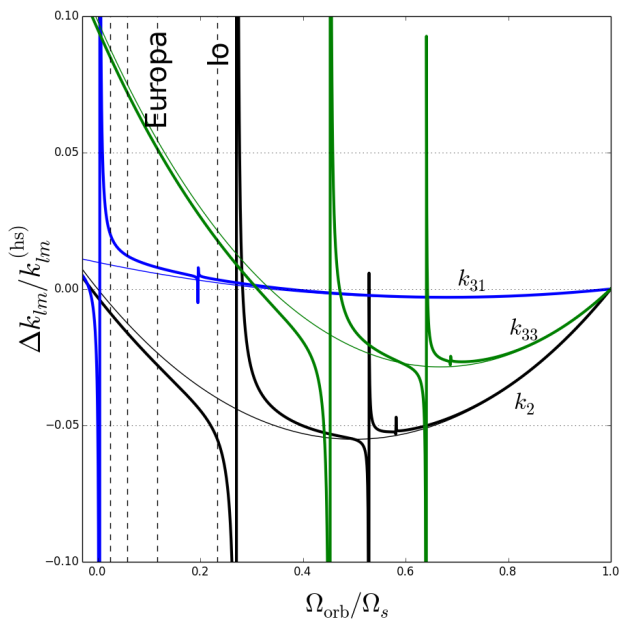


Figure 4. Same as Fig. 2, but for the $n = 1$ model with stable stratification in two regions: $r/R \in [0.5, 0.7]$ and $[0.85, 0.93]$.

0.025) and $\Gamma_1 = \Gamma = 1 + 1/n$ otherwise, i.e.,

$$\Gamma_1(r) = 2 + \frac{0.4}{[1 + e^{40(\bar{r}-0.7)}][1 + e^{-40(\bar{r}-0.5)}]} \quad (26)$$

(iii) $\Gamma_1 = 2.4$ only in two stable regions $\bar{r} = r/R \in [0.5, 0.7]$ and $[0.85, 0.93]$ (with a transition width of 0.025) and $\Gamma_1 = \Gamma = 1 + 1/n$ otherwise (see Table 1).

For each model, we compute the f-modes and g-modes of a nonrotating planet (see Table 1), and use Eqs. (12)-(13) to account for the effect of rotation on the modes. We include only the first three radial-order g-modes in our calculation of k_{lm} . The perturbative approach of the rotational effect is approximately valid for these modes since $mC\Omega_s$ is less than the mode frequency $|\omega_0|$.

Figures 2-4 show the results for the dynamical Love numbers based on the three models. It is obvious that significant dynamical correction to the hydrostatic $k_{lm}^{(hs)}$ occurs around the resonance, where $\omega_\alpha = \omega$. The “strength” of each resonance is measured by the tidal overlap coefficient, and a large $|Q_t|$ value implies that the “width” of the resonant feature is larger (see Eq. 16). For the $\Gamma_1 = 2.4$ model, the stratification is strong,

the broad/strong resonance with the g_1 mode can affect k_{lm} associated with the Galilean moons (Fig. 2). For the model with the stable stratified region restricted to $r/R \in [0.5, 0.7]$ (Fig. 3), the resonance feature is much weaker/narrower, but still $\Delta k_2/k_2^{(hs)}$ becomes -5% for Io. When the model further includes the stratified region at $r/R \in [0.85, 0.93]$ (Fig. 4), the resonance features shift and broaden, and k_{31} becomes affected for the Galilean moons. Obviously, these results are for illustrative purpose, but they indicate that resonance features due to stable stratification in the planet’s interior may influence the the measured dynamical Love numbers.

Note that Figures 2-4 do not include contributions from high-order g-modes. These modes (with mode frequencies comparable to Ω_s) become mixed with inertial modes (so-called “inertial-gravity” modes; see Xu & Lai 2017) and cannot be treated using Eqs. (12)-(13). However, because of their small tidal overlap coefficients, they are unlikely to be important contributors to k_{lm} except for the coincidence of an extremely close resonance.

6. CONCLUSION

We have derived a general equation (Eq. 11) for computing the dynamical Love number k_{lm} of a rotating giant planet in response to the tidal forcings from its satellites. In most situations, the Love number is dominated by the tidal response of f-modes, and the general expression reduces to Eq. (16), which can be easily evaluated using the mode properties of nonrotating planet models (see Table 1). We show that the 4% discrepancy between the measured k_2 of Jupiter and the theoretical hydrostatic value can be naturally explained by the dynamical response of Jupiter’s f-modes to the tidal forcing from Io – the key is to include the rotational (Coriolis) effect in the tidal response in a self-consistent way. We also show that the contributions of the inertial modes to the Love number k_2 are negligible.

We have also explored the effect of stable stratification in Jupiter’s interior on the Love numbers. If sufficiently strong stratification exists in a large region of the planet’s interior, g-mode resonances may influence the dynamical Love numbers associated with the tidal forcing from the Galilean moons. Thus, precise measurements of various k_{lm} could provide constraints on the planet’s interior stratification.

REFERENCES

- Debras, F., & Chabrier, G. 2019, *Astrophys. J.* 872, 100
 Durante, D., et al. 2020, *Geophysical Research Letters*, 47, e2019GL086572
 Friedman, J.L., & Schutz, B.F. 1978, *Astrophys. J.* 221, 937
 Ho, W.C.G., & Lai, D. 1999, *MNRAS*, 308, 153

- Idini, B., & Stevenson, D.J. 2021, PSJ, in press
(arXiv:2102.09072)
- Lai D., & Wu, Y. 2006, Phys. Rev. D 74, 024007
- Schenk, A.K. et al. 2002, Phys. Rev. D 65, 024001
- Stevenson, D.J. 2020, AREP, 48, 465
- Unno, W., et al. 1989, Nonradial oscillations of stars,
University of Tokyo Press
- Wahl, S. M., et al. 2017, Geophys. Res. Lett. 44, 4649
- Wahl, S. M., Parisi, M., Folkner, W. M., Hubbard, W. B.,
& Militzer, B. 2020, The Astrophysical Journal, 891, 42
- Xu, Wenrui, & Lai, D. 2017, Phys. Rev. D 96, 083005